A MULTI-TEMPORAL ANALYSIS OF VEGETATION DYNAMICS
IN THE IBERIAN PENINSULA USING MODIS-NDVI DATA

Ana Pérez-Hoyos, Beatriz Martínez, María Amparo Gilabert and Francisco Javier García-Haro

Departament Física de la Terra I Termodinámica, Universitat València,
C/Dr. Moliner, 50. 46100 Burjassot, Valencia, Spain; ana.perez-hoyos(at)uv.es

ABSTRACT

The aim of this study is to characterise the vegetation dynamics of the Iberian Peninsula using MODIS-NDVI time series (2000-2008) at 1 km resolution. For this purpose, *NDVI* profiles are analysed using filtered data derived from a spectral technique, a multi-resolution analysis (MRA) based on the wavelet transform (WT). The MRA results in an additive decomposition of the time series into several components associated with variations on a particular temporal scale. First, the functional diversity of the Iberian Peninsula is described by using several metrics derived from the first component of the MRA (filtered time series). Second, a trend analysis is performed with the fifth component of the MRA having a semi-period around a year (inter-annual component) in order to detect potential vegetation changes over the considered period. The 3-month scale Standard Precipitation Index (*SPI*-3) was used to better identify changes. As a result of the functional diversity a characterisation of the Ecosystem Function Types (EFT) of the Iberian Peninsula with 30 representative classes is obtained. The EFT present a decreasing northwest to southeast biomass gradient. An exploratory analysis with the CORINE land cover classification revealed the importance of land cover in explaining the functioning of particular ecosystems, particularly for ecosystems showing a strong seasonal dynamics, such as rice and non-irrigated crops. Finally, the trend analysis indicates that most vegetation changes over the considered period are due to forest fires and are connected to the *SPI* trend.

INTRODUCTION

Terrestrial ecosystems are constantly changing on a wide range of both spatial and temporal scales as a consequence of natural and/or anthropogenic factors. Quantifying the magnitude of land-cover change is crucial to understand the ecosystem dynamics. Satellite remote sensing has long been considered an ideal technology for this purpose because it permits analyses of large areas with a high temporal frequency. With new sensors like MODIS (MODerate resolution Imaging Spectroradiometer), new data are available to extract key phenological parameters and monitor trends in vegetation dynamics (1).

Normalised difference vegetation index (*NDVI*)-based time series have been broadly used to track global vegetation because they are very good descriptors of vegetative phenology. Several methodologies have been developed to monitor vegetation dynamics from multi-temporal data such Harmonic analysis (2), Fourier trend analysis (3) and, most recently, Wavelet decomposition (4,5). Wavelet Transform (WT) uses local basis functions (wavelets) that can be stretched and translated with a flexible resolution in both frequency and time domains. WT can be understood as a technique that looks at different sections of the time series with a window adjusted according to scale. Thus, a narrow window can be used to capture the presence of short-lived events (high frequency variability), such as abrupt changes, while still resolving processes that show low frequency variability in time scale. This procedure, which is known as multi-resolution analysis (MRA) (6), has shown to be an adequate tool to decompose the *NDVI* time series into different temporal components (e.g. inter and intra-annual), thus allowing us to characterise the vegetation dynamics (4,7).

Different attributes of the annual average *NDVI* curve have been derived to capture the mean characteristics of the seasonal dynamics of carbon gains (8), such as annual integral (*INDVI*), the relative annual range (*RREL*) and the date of maximum *NDVI* (*MMAX*). These attributes are the

main input variables to obtain Ecosystem Functional Types (EFT), which can be defined as a group of ecosystems sharing functional characteristics that include the amount and timing of matter and energy exchanged between the biotic community and the environment. Previous studies carried out in the study area with AVHRR data show that the dynamics of primary production is a good functional variable to define EFT (9).

The aim of this study is to characterise the vegetation dynamics of the Iberian Peninsula using 16-day MODIS *NDVI* time series at 1 km spatial resolution over the period 2000-2008. For this purpose, different temporal components derived from the multi-resolution analysis (MRA) are considered. First, the functional diversity of the Iberian Peninsula is described by defining EFT using a filtered time series component derived from the MRA. Second, a trend analysis is performed on the inter-annual component derived from the MRA in order to detect vegetation changes over the considered period.

STUDY AREA AND MATERIAL

Study area

The Iberian Peninsula has a dimension of 582 860 km^2 and is highly heterogeneous in landscape, climatic conditions and relief, thereby comprising a wide range of ecosystems. The orography of the study area, with elevation ranging from sea level to 3 479 m, plays an important role in the climate of each region, and shows a high variability from North to South and from East to West. The main land cover is non-irrigated land, principally located in a vast central plateau surrounded by a number of mountain ranges that together with the Pyrenees are covered with natural land cover such as shrubland, broadleaved and coniferous forests.

NDVI data

The 16-day MODIS *NDVI* product (MOD13A2) at 1 km spatial resolution has been used to perform the multi-temporal analysis over the Iberian Peninsula for a 9-year period, from February 2000 to December 2008. This product provides a consistent spatial and temporal dataset for monitoring global vegetation conditions. MOD13A2 uses MODIS surface reflectances, corrected for molecular scattering, ozone absorption, aerosols, and *BRDF* adjusted to a nadir angle (10). The tiled *NDVI* data were first mosaicked, then re-projected from the Sinusoidal to Geographic (Lat/Lon) WGS84 projection, and finally stacked to produce the time-series data set. The associated quality flag was used to discard pixels with significant cloud or snow/ice presence and gaps were filled using a linear interpolation method.

SPI data

In order to assist in a more comprehensive identification of the land-cover changes, a drought index such as the Standardised Precipitation Index (*SPI*) has been considered. In this study, monthly climatic maps of precipitation were derived over Spain for the 1950-2008 period at a 2 km spatial resolution using geostatistical approaches for interpolation (11). The climatic data used in the study were obtained from the Agencia Estatal de Meteorología (AEMet) and correspond to 2500 to 4800 recording stations (depending on the period) distributed through Spain. The *SPI* is calculated by fitting historical precipitation data to a Gamma probability distribution function from a specific time period and location, and transforming the Gamma distribution to a normal distribution with a mean of zero and standard deviation of one (12). The *SPI* can be calculated and analysed using multiscale depending on the focus of a study. In this study, the 3-month *SPI*, which provides a seasonal estimation of precipitation, is calculated taking into account the precipitation total of the current month and previous 2 months.

EXPERIMENTAL PROCEDURE

The MRA applied to time series

The fundamental idea behind wavelets is to analyse the signal according to different time scales or resolutions. In case of the multi-resolution analysis (MRA), a discrete wavelet transform (DWT)

may be implemented in a hierarchical algorithm, well known as pyramid algorithm (13). The DWT, specifically adapted for discrete signals, allows for a decomposition of the signal into time scales based on powers of two, also known as a dyadic sampling. As a result of the MRA, the original signal $f(t)$ can be reconstructed as:

$$f(t) = A_m(t) + \sum_{j=1}^{m} D_j(t)$$ (1)

where m is the highest decomposition level considered, A is the approximation component and D the detail component. In the first level of the decomposition, $f(t)=A_1+D_1$, the signal has a low-pass filtered component, A_1, and a high-pass filtered component, D_1. In a second step, the approximation A_1 is split as $A_1=A_2+D_2$, and so on. The relationship $D_j=A_{j-1}-A_j$, gives us information about the portion of the signal that can be attributed to variations between the scales [j-1, j], whereas the A_m component is associated with averages over scales 2^m and longer and, therefore, captures the slowly varying portion of the original signal (14).

Several wavelets functions can be found in the literature with different characteristics. In our case, the Meyer orthogonal discrete wavelet (15) has been chosen. It has demonstrated successful results in land-cover changes analyses from time series of MODIS images (16) and AVHRR *NDVI* imagery (4). Table 1 shows the period and semi-period corresponding to the different MRA scales for the Meyer wavelet, with a centre frequency of 0.67213 Hz and a sampling period of 16 days (as in our *NDVI* time series). The WT can be interpreted in terms of differences between temporally adjacent averages over the studied time range at different scales. Thus, it seems most appropriate to select the time scale corresponding to the semi-period since the inter- and intra-annual components should account for differences between years and months, respectively (4). Two relevant outputs for our study are: 1) the filtered time series, A_1, which refers to the component of the signal whose noise due to the temporal scale below one month has been removed, and 2) the A_5 component or inter-annual component which reflects changes over time scales of 380 days and longer, allowing us to detect the presence of a long-term variation in the considered period.

Table 1: Period and semi-period corresponding to the different MRA scales for the Meyer wavelet.

Level (*j*)	Scale (*a*)	Frequency (Hz)	Period (day)	Semi-period (day)
1	2	12.2840	47	23.5
2	4	6.1423	95	47.5
3	8	3.0711	190	95
4	16	1.5356	380	190
5	32	0.7678	760	380

Methodology

The experimental procedure to study vegetation dynamics using MRA is divided into two steps. First, a functional diversity analysis of the Iberian Peninsula is performed using the filtered time series A_1. Then, the metrics *INDVI*, *RREL* and *MMAX* are computed from the A_1 averaged year. Based on these metrics, and following the methodology suggested by (17), an EFT map for the Iberian Peninsula is derived. Different codes are assigned to each EFT based on two letters and a number. The first letter of the code corresponds to the *INDVI* level, ranging from *A* (low) to *D* (high). The second letter (small) indicates *RREL*, ranging from *a* (low) to *d* (high values). The numbers indicate the season of maximum *NDVI*. In order to define the intervals (Table 2), the histogram of each variable has been obtained and the 25, 50 and 75 percentiles are chosen as cut-off points for the intervals. In the case of date of maximum, four intervals are defined which are in close correspondence with the four seasons that occur in a temperate ecosystem (8). As a result, a total of 64 EFT classes are defined for the whole Iberian Peninsula.

Second, a non-parametric Mann-Kendall trend analysis (e.g., *tau-b* coefficient, significance and *p*-values) of the series is performed using the A_5 component. This is a widely used rank order based test which is insensitive to missing values, easy to calculate and robust against non-normality (18). The Mann-Kendall test is an indicator of the strength and direction of a trend but it is insensitive to

its magnitude. Hence, the slope Q of the trend is determined by means of Sen's non-parametric method (19).

Table 2: Range of the functional traits used in the definition of ecosystem functional types (EFTs).

	Functional code
INDVI	*A* (0.001- 0.351)
NDVI Annual Integral	*B* (0.351- 0.459)
Sum of positive *NDVI* values over a year	*C* (0.459- 0.563)
	D (0.563- 0.872)
RREL	*a* (0.026- 0.279)
Relative Range of *NDVI*	*b* (0.279- 0.455)
$\dfrac{NDVI_{max} - NDVI_{min}}{INDVI}$	*c* (0.455- 0.722)
	d (0.722- 2.77)
MMAX	1 (Summer: July, August, September)
Month of the Maximum *NDVI*	2 (Autumn and early winter: September, October, November)
Date when the maximum *NDVI* value occurs	3 (Late winter and early spring: January, February, March)
	4 (Late spring: April, May, June)

RESULTS

Functional diversity of the Iberian Peninsula

Using the annual averaged *NDVI* curve as input, the relevant attributes (*INDVI*, *RREL* and *MMAX*) were computed (Figure 1a-c). A clear and contrasting pattern across the Iberian Peninsula is observed. The date of the maximum *NDVI* is related to the phenological cycle of each vegetation type, thus the spatial distribution of this variable (Figure 1a) is closely related to the land cover distribution. Two peaks of vegetation activity are recorded, one in April (23.1%) and the other in December (12.7%). Areas corresponding to high values in April are located in the central plateau and are mainly covered by non-irrigated crops while the winter peak corresponds to citrus crops in the eastern coastal area.

INDVI decreases gradually from the northwestern part of the study region toward the southeast, with the exception of the broadleaved forest located in the central part of the southern coast (Figure 1b). Forested areas have the largest INDVI (values near 0.8) indicating the high volume of green biomass persistent throughout the year. Extreme values about 0.2 correspond to areas of sparse vegetation such as the desert of Tabernas in the southeast and rugged areas (e.g. Pyrenees). The rest of the study area is dominated by cultivated areas, with values around 0.3 and 0.4. The values in the west are slightly higher than those in the east, where the rainfall is low and has a direct impact on vegetation growth.

The relative range (Figure 1c) shows an opposite pattern to *INDVI*. Northwest forested areas with abundant vegetation throughout the year have a low intra-annual variation. In contrast, areas with low *INDVI* values usually present more variability in the total amount of vegetation during the year (with the exception of sparse vegetation) and therefore a higher relative range. These areas present a low level of NDVI in winter and a rapid increase in spring or summer, as in the case of rice fields and annual crops.
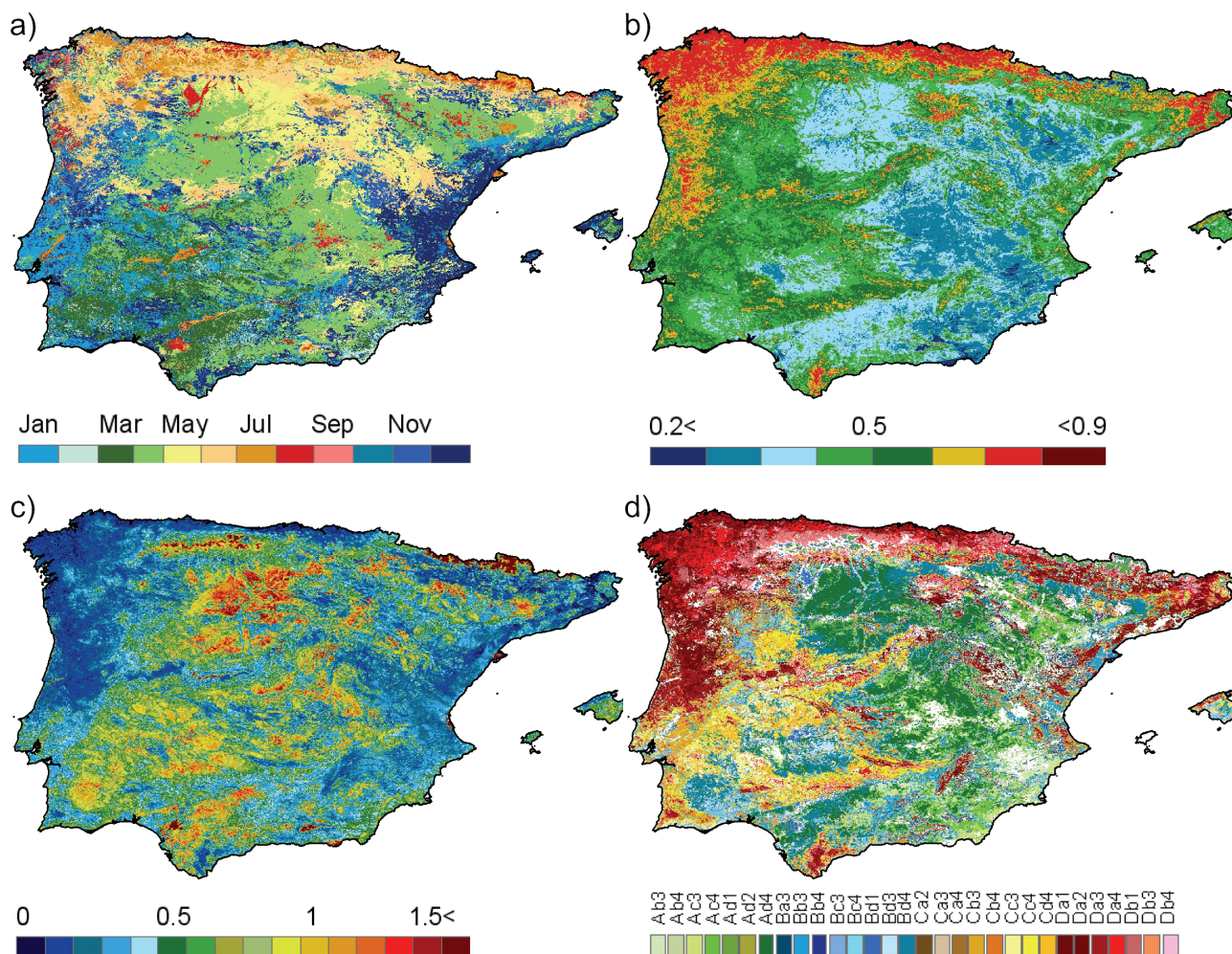
Figure 1: a) Month of Maximum (MMAX), b) Relative Range (RREL), c) INDVI (NDVI Annual Integral), d) Ecosystem Functional Types (EFTs).

Figure 1d shows the EFT derived from the *NDVI* metrics. EFT with less than 1% in coverage are not considered (marked in white colour). In fact, some theoretical EFT are inexistent because of biophysical restraints. An example would be Dd1, presenting high biomass and high seasonal variability. As a result, only 30 classes of the initial 64 are represented. Dominant EFT are Ad4 and Bd4, with a percentage of 9.4% and 7.6%, respectively. These ecosystems only differ in the amount of biomass and are dominated by late spring maximum with a higher intra-annual variability such as non-irrigated areas. Irrigated crops and rice fields are shared by the same EFT (Bd1), with high intra-annual variability and a summer peak. This is an example of different land cover classes having a similar primary production. Northern forested areas are mainly composed of high productivity and low seasonality classes (Da1, Da4), while broadleaved forests in southwest Portugal have less biomass and little annual variation (Cb4) as a consequence of a minor rainfall.

The correspondence between functional units and land cover is also analysed using CORINE land cover as a reference. The original CLC2000 dataset (100 m resolution) was resampled over a grid at 1 km and degraded to 18 classes (Figure 2a). A visual inspection confirms previous findings. For example, ecosystems with high biomass productivity in the north (red colours in Figure 1d) are primarily *Broadleaf forest* and *Transitional wood-land,* while EFT with low productivity (green colours) are associated with semiarid areas of south-eastern Iberia, occupied by *Sparse vegetation* or *Cultivated and managed areas.*

Cross-tabulation and boxplot analyses (not shown for brevity) were performed to evaluate the association between EFT and specific land covers. For example, the Ad1 unit includes 90% of the rice fields, whereas Ad4 and Bd4 include the majority of non-irrigated land. In general, land covers

showing a higher seasonal dynamics show a clear correspondence with EFT. Therefore, it can be observed that there are different functional units within the same land cover and vice versa. This is mainly caused by the fact that the schemes of classification differ in criteria. Results point out the importance of land cover in explaining the functioning of particular ecosystems.
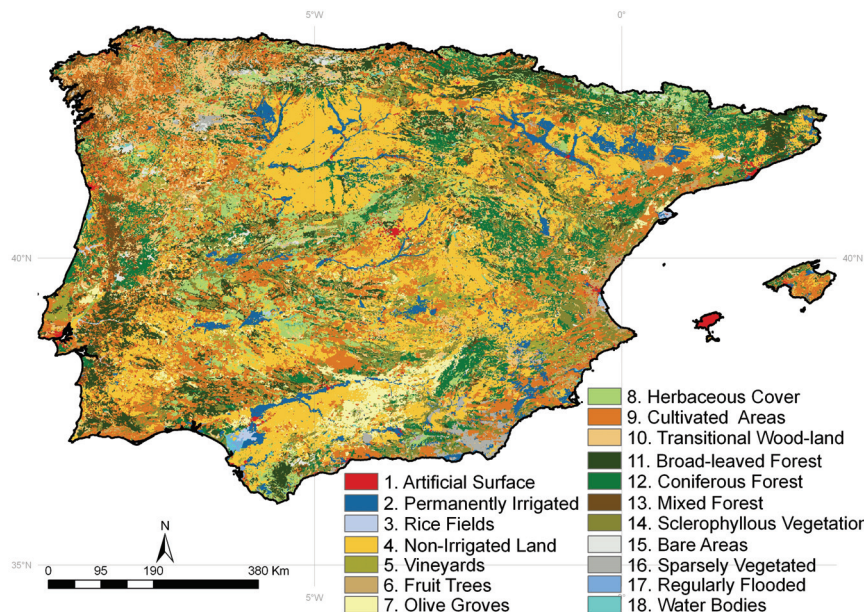

Figure 2: CORINE land cover.

Trend analysis

The trend analysis was performed by calculating the slopes (*Q*) of the inter-annual AGC component (Figure 3a). Positive and negative slopes are depicted in green and red colours, respectively, whereas non-significant slopes appear in white. The Standardised Precipitation Index (*SPI*) trend for the considered period was obtained after applying the Sen´s slope to the inter-annual *SPI* component derived from the MRA. Figure 3b shows the significant *SPI* changes for Spain. The rainfall pattern agrees with that established by other authors (20) and information derived from AEMet for the period 2000-2008. Lowest values (red colours) are observed in the north and north-western Spain due to a drought period during 2003. On the contrary, highest values (green colours) are observed in the east and south-eastern Spain mainly due to a moderate increase of precipitation in 2006 and a significant rainfall excess in 2007 and 2008.

Only strong negative *NDVI* are rather local in this map and mostly coincide with forest fires that occurred during the studied period. These areas seem to be widespread on the Iberian Peninsula within the observation period corresponding to negative *SPI* trends (rainfall deficits). Table 3 summarises the occurrence and burnt area of those forest fires identified in the image. Some large burnt areas well identified in the image are localised in the provinces Huelva and Sevilla (I), Guadalajara (II), La Coruña and Pontevedra (III), and in Portugal (VI, VII). According to the Ministerio de Medio Ambiente y Medio Rural (MARM) of Spain, 2000, 2005 and 2006 were the years with the most fire-affected areas (> 155 000 ha). In particular in 2006, Spain was the European country with the largest fire-affected areas with Galicia being the most affected province (> 76 000 ha burnt area).

In the case of Portugal, it faced in 2003 the worst fire season ever recorded followed by 2005. From Figure 3a it is possible to identify recurrent burnt areas (> 125 000 ha) in the districts of Castelo Branco, Portalegre, Santarén and Coimbra. In 2003, the affected district of Faro in the south of Portugal and the district of Viana do Castelo, Braga and Porto in 2006, are also detected (21)**.**

Regarding the positive trends, the dominance of an increase in *NDVI* along the Mediterranean coast is noticeable. Most of the positive trends coincide with areas where a forest fire occurred at the beginning or just before the considered period. This is the case of Cabo de Creus (the northwest part of Cataluña (A in Figure 3a) and Simat southeast of Valencia (B in Figure 3a), which

were affected by an intensive fire in 2000. Other highly affected areas in Valencia province are around Requena, Buñol and Enguera towns (B), which have been affected by frequent forest fires, (fire damaged around 140 000 ha in 1994). In all these cases, a gradual increase in the vegetation is observed after the fires revealing a post-fire vegetation recovery. The rate of recovery is especially high due to the significant rainfall excesses observed along the Mediterranean Coast during the considered period.
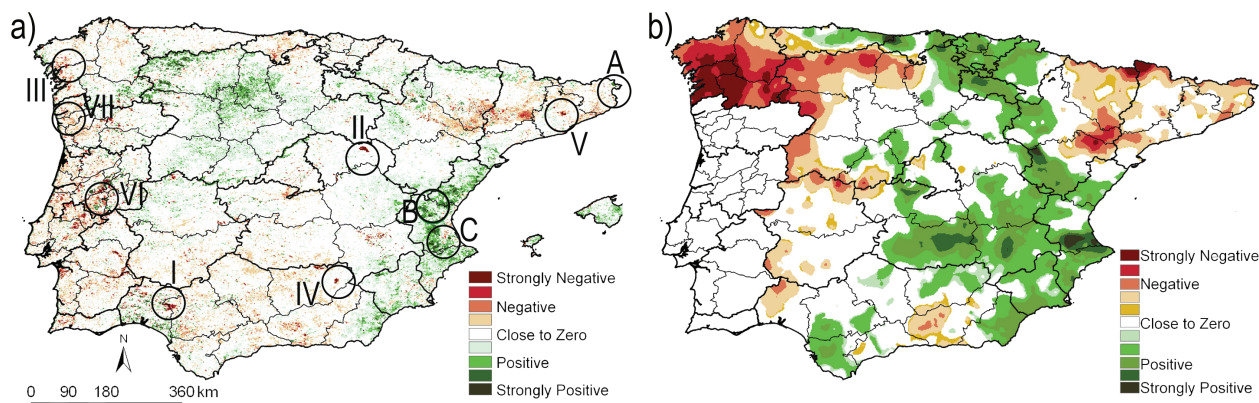

Figure 3: a) Slope of the approximation time series (A_5) b) Slope of SPI for 2000-2008.

Table 3: Main Forest Fires in the Iberian Peninsula over the period (2000-2008).

Forest Fire	Country	Province	Date	Burnt Area (ha)
I	Spain	Huelva/ Sevilla	July 2004	> 28 000 ha
II	Spain	Guadalajara	July2005	> 13 000 ha
III	Spain	La Coruña/ Pontevedra	August 2006	> 76 000 ha
IV	Spain	Jaén	August 2005	> 5 000 ha
V	Spain	Barcelona	August 2003	> 3 000 ha
VI	Portugal	Castelo Branco/ Portalegre/ Satnerén/ Coimbra	2003/ 2005	> 125 000 ha
VII	Portugal	Viana Do Castelo	2006	> 30 000 ha

** Information provided by the Ministerio de Medio Ambiente of Spain.
 * Information derived from the European Commission (http://ies.jrc.ec.europa.eu).

CONCLUSIONS

This work uses a multi-resolution analysis (MRA) based on wavelet transform (WT) to study vegetation dynamics from MODIS *NDVI* data (2000-2008) in the Iberian Peninsula. Two components of the wavelet transform, A_1 and A_5, reveal interesting aspects of the vegetation dynamics. Firstly, different key features (*INDVI*, *RREL* and *MMAX*) can be calculated based on the component A_1, which reduces noise in the data. The EFT derived from *NDVI* metrics show a decreasing biomass gradient from northwest to southeast in the Iberian Peninsula. Northern areas covered by broadleaf forests present ecosystems with high biomass and low intra-annual variability (Da4, Da1). Southwest areas with dominance of sparse vegetation present functional ecosystems with low biomass and high intra-annual variability (Ac3). The dominant EFT, Ad4 (9.4%) and Bd4 (7.5%), occupy the central area of the peninsula, and are closely related to crop areas with low biomass, high intra-annual variability and peaks in late spring. An exploratory analysis of EFT in relation to CORINE land cover has revealed that those land covers which have a wide range of seasonal dynamics are more closely related to ecosystem functioning.

Secondly, the inter-annual component A_5 is used to detect trends in the data series. Main results show that negative changes coincide with forest fires that occurred during the period studied. These areas are also consistent with rainfall deficits observed in the *SPI* trend image. Positive trends, mainly located along the Mediterranean coast, coincide with areas where the vegetation recovery after forest fires is being influenced by significant rainfall excesses.

REFERENCES

1   Galford G L, J F Mustard, J Melillo, A Gendrin, C C Cerri & C E P Cerri, 2008. Wavelet analysis of MODIS time series to detect expansion and intensification of row-crop agriculture in Brazil. Remote Sensing of Environment, 112 (2): 576-587

2   Verhoef W, M Menenti & S Azzali, 1996. A colour composite of NOAA-AVHRR-NDVI based on time series analysis (1981-1992). International Journal of Remote Sensing, 17(2): 231-235

3   Azzali S & M Menenti, 2000. Mapping vegetation-soil-climate complexes in southern Africa using temporal Fourier analysis of NOAA-AVHRR data. International Journal of Remote Sensing, 21: 973-996

4   Martínez M & M A Gilabert, 2009. Vegetation dynamics from NDVI time series analysis using the wavelet transform, Remote Sensing of Environment, 113(9): 1823-1842

5   Sakamoto T, M Yokozawa, H Toritani, M Shibayama, N Ishitsuka & H Ohno, 2005. A crop phenology detection method using time-series MODIS data. Remote Sensing of Environment, 96: 366-374

6   Burke-Hubbard B, 1998. The World According to Wavelets. The Story of a Mathematical Technique in the Making (A K Peters, 2nd edition) 330 pp.

7   Percival D B, M Wang & J E Overland, 2004. An introduction to wavelet analysis with application to vegetation monitoring. Community Ecology, 5: 19-30

8   Zhang X, M A Friedl, C B Schaff, A H Strahler, J C F Hodges, F Gao, B C Reed & A Huete, 2003. Monitoring vegetation phenology using MODIS. Remote Sensing of Environment, 84: 471-475

9   Alcaraz D, J Paruelo & J Cabello, 2005. Identification of current ecosystem functional types in the Iberian Peninsula, Global Ecology and Biogeography, 15: 200-212

10 Huete A, C Justice & W V Leewen, 1999. MODIS Vegetation Index (MOD13), Algorithm Theorical Basis Document Version 3 (University of Virginia) 120 pp. http://modis.gsfc.nasa.gov/data/atbd/atbd_mod13.pdf (last date accessed: 18 Aug 2010)

11 Goovaerts P, 1997. Geostatistics for Natural Resource Evaluation (Oxford University Press) 464 pp.

12 McKee T B, N J Doesken & J Kleist, 1993. The relationship of drought frequency and duration to time scales. In: Proceeding of the 8th Conference on Applied Climatology (American Meteorological Society, Boston) 179-184

13 Mallat, S, 1989. A theory for multiresolution signal decomposition: the wavelet representation. IEEE Transactions on Pattern Analysis and Machine Intelligence, 11, 674-693

14 Percival D B & A T Walden, 2000. Wavelet methods for time series analysis (Cambridge University Press) 594 pp.

15 Abry P, 1997. Ondelettes et turbulence (Diderot) 268 pp.

16 Freitas R M & Y E Shimabukuro, 2008. Combining wavelets and linear spectral mixture model for MODIS satellite sensor time-series analysis. Journal of Computational Interdisciplinary Sciences, 1: 33-38

17   Paruelo J M, E G Jobbágy & O E Sala, 2005. Current distribution of ecosystem functional types in temperate South America. Ecosystems, 4: 683-698

18   De Beurs K M & G M Henebry, 2005. A statistical framework for the analysis of long image time series. International Journal of Remote Sensing, 25: 1551-1573

19   Sen P K, 1968. Estimates of the regression coefficient based on Kendall's tau. Journal of the American Statistical Association, 63: 1379-1389

20   Poquet D, F Belda & F J García-Haro, 2008. Clasificación Topoclimática de la Sequía en la Península Ibérica de 1950 a 2007 a partir del SPI. In: VI Congreso Internacional de la Asociación Española de Climatología, Tarragona, 8-11 October 2008

21   Schmuck G, J San-Miguel-Ayanz, P Barbosa, A Camia, J Kucera, G Libertá, G Amatulli & R Boca, 2006. Forest Fires in Europe. Scientific and Technical Report of the European Commission, EUR 22931 EN, JRC37598
     http://effis.jrc.ec.europa.eu/reports/fire-reports/doc/2/raw (last date accessed: 18 Aug 2010)